Science of Sintering, **53** (2021) 79-90

https://doi.org/10.2298/SOS2101079A

UDK: 615.464; 677.017.5; 676.017.2

Development of Optical, Microstructural and Mechanical Properties of Porcelain Stonewares

Tuna Aydin[1*)], Osman Bican[1], Recep Gümrük[2], Hamdi Kuleyin[3]

[1]Kirikkale University, Engineering Faculty, Metallurgy and Material Engineering Department, Kirikkale, Turkey

[2]Karadeniz Technical University, Mechanical Engineering Department, Trabzon, Turkey

[3]Recep Tayyip Erdogan University, Mechanical Engineering Department, Rize, Turkey

Abstract:

New production systems developed in recent years made it possible to improve different aesthetic appearance and large sizes for porcelain stonewares. In order to produce these tiles, optical and mechanical properties of the porcelain stonewares should be improved. Optical and mechanical properties also related with microstructure. In this study, spodumene, alumina and zircon were used to improve the microstructure of the porcelain stonewares and consequently their optical and mechanical properties. The wear resistance of porcelain stonewares is the one of the most important mechanical properties. In this study, a different test method was used because the existing wear test methods on the tiles were insufficient. The solid particle impingement method using alumina particles was used to determine wear resistance of the porcelain stoneware bodies.

Keywords*: Porcelain stoneware; Solid particle impingement; Wear resistance; Optical properties.*

1. Introduction

Porcelain stonewares have a wear resistance test method used as standard (ISO 10545-5 and 10545-6). However, this method is inadequate especially in porcelain stoneware products. For this reason, most of the tile manufacturers offer their own test methods in addition to the standard test. This article introduces a new perspective for wear resistance. Porcelain stonewares are made of clay, quartz, kaolin and feldspar. The white porcelain stonewares also contain zircon ($ZrO_2.SiO_2$) and alumina (Al_2O_3) due to the whiteness and mechanical properties of these raw materials [1, 2]. Porcelain stoneware bodies with superior surface mechanical characteristics, chemical resistance and whiteness were obtained using zircon and alumina powders. Due to the excellent chemical and wear resistance and high hardness properties of these powders, these raw materials were used in this study [2, 3]. Zircon ($ZrO_2.SiO_2$) is also used as an opacifier due to its opacifying effect in porcelain stoneware production [1]. Opacity is the result of the difference between the refractive index of an opacifier and that of matrix. As the difference between the refractive indexes of the opacifier and that of matrix increases, more satisfactory opacity can be obtained. Also, the

*) **Corresponding author:** tunaaydin@kku.edu.tr

increase in the number of crystals increases the number of reflective surfaces that increase the opacity of the body [1-4]. Alumina has remarkable mechanical properties. Especially, there are lots of advantages on strength characteristics for high or low-alumina porcelains [5]. Alumina has also a good opacifying properties due to their higher than average refractive indices [6]. New production systems made it possible to improve aesthetic appearance and large sizes for porcelain stonewares. In order to improve aesthetic appearance and large sizes, optical and mechanical properties of the porcelain stonewares should be improved.

In this study, it was investigated to effect of alumina and zircon powders on optical and mechanical properties of porcelain stonewares. Optical properties were improved using zircon. Mechanical properties were improved using alumina and spodumene. The decrease in liquid phase viscosity at higher temperature resulted from spodumene addition. The decrease in the viscosity contributed to rise up in the amount of mullite and the growth of mullite crystals [7, 8]. In this study, the presence of alumina, zircon and mullite crystals provided the improvement of mechanical properties.

2. Materials and Experimental Procedures

Clay, kaolin, feldspar and quartz were used for producing standard (STD) body. Alumina and zircon was also used to investigate the effect of these materials on optical and mechanical properties of porcelain stoneware. After grounding process, uniaxial press was used to form granules in a 5 cm × 10 cm die. The press pressure is 450 kg/cm^2. Drying process was performed at 110 °C. All samples were fired at 1210 °C for 60 min (Carbolite CWF 12/13). XRF was used for analysing of the chemical compositions (Rigaku, ZSX Primus XRF). X-ray diffraction (XRD) was used for phase analyses of the fired samples between 5º to 55° (with CuKα radiation, Rigaku Rint 2200, scanning speed of 2°/min). MAUD software programme was used for analysing Quantitative phase analyse. In order to determine microstructural properties the scanning electron microscope was used (SEM, Zeiss EVO 50EP). The bulk densities and the total porosities of the samples were obtained from Helium pycnometer (Quantachrome Model MVP-1 Multipycnometer) and Archimedes method. The mechanical properties such as, hardness, elastic modulus, wear behaviours and bending strength were investigated. The elastic module was determined using ultrasonic test method (Olympus Panametrics Model 5800 Computer Controlled Pulsar/Receiver, Tektronix TDS 1012 Two Channel Digital Storage Oscilloscope) [8]. Micro-hardness tests were performed on fired samples, at the indentation loads of 0.96 N (Galileo Durametria, Viskers HV1 OD). The wear resistance measurements of porcelain stonewares were carried out by particle/sand erosion testing method using alumina sand (Fig. 1).

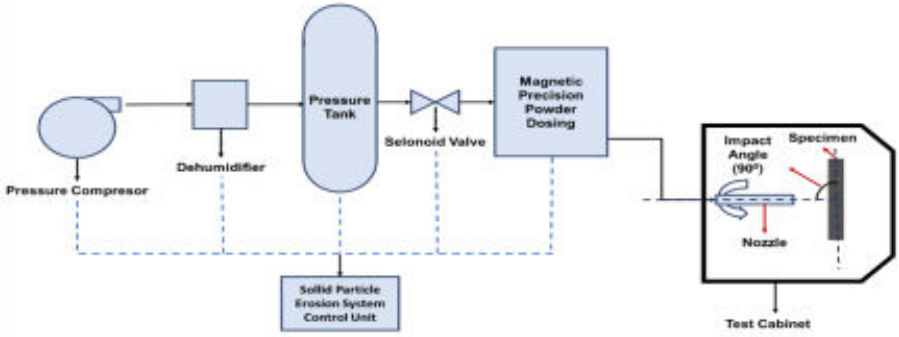

Fig. 1. Schematic figure of solid particle erosion test system.

The diameter of Alumina particle is 50 μm. The velocity and the flow rate of the alumina sand are 74 m.s^{-1} and 2.5 gr.min^{-1} respectively [8]. In this study, the different impact angles (30º,

45º, 60º and 90º) were used. The test was conducted according to ASTM G76-13 standard. Vickers hardness measurements were conducted using HV0.2, and load (0.5 kgf). Hardness test was carried under the laboratory conditions on GALILEO Digi25R Vickers tester.

3. Results and Discussion

3.1. Chemical analysis

As can be seen in Table I, STD body is made of Na feldspar, quartz, two type of kaolin and three type of clay. SW1, SW2 SW3 and SW4, made of clay B, kaolin A, sodium feldspar, quartz, zircon, alumina and spodumene. Spodumene was also used at a ratio of 1 and 2 % in this study. Spodumene was used instead of Na-feldspar. SW1 contains clay, kaolin B, quartz, sodium feldspar, zircon, and alumina. SW2 is made of clay B, kaolin B, quartz, sodium feldspar, zircon, and alumina. Spodumene was also used in SW2 in a ratio of 1wt%. instead of sodium feldspar. SW3 is made of clay A, kaolin A, clay B, sodium feldspar, zircon, alumina and spodumene. SW4 body contains spodumene in a ratio of 2wt%. instead of sodium feldspar. SW2, SW3 and SW4 bodies do not contain any quartz content. Table II shows Seger oxide ratios. As seen on Table II, the opacity increased with addition of alumina and zircon. The opacity value of the samples was calculated by correlating seger molar ratios and refraction index of Al_2O_3 and ZrO_2.

Tab. I Chemical compositions of raw materials.

	Lol.*	SiO_2	Al_2O_3	Fe_2O_3	TiO_2	CaO	MgO	Na_2O	K_2O	Li_2O	ZrO_2
Kaolin A	10.01	65.01	23.0	0.500	0.500	0.200	0.150	0.200	0.300	-	
Quartz	0.430	97.63	0.730	0.180	0.030	0.100	0.010	0.011	0.470	-	
Na Feldspar	0.501	71.11	17.400	0.051	0.240	0.600	0.101	9.360	0.340	-	
Clay A	10.000	59.01	26.0	1.200	1.500	0.600	0.100	0.100	2.00	-	
Clay B	8.500	59.01	25.00	1.000	1.500	0.600	0.700	0.600	2.70	-	
Clay C	7.500	65.00	21.50	2.500	1.300	-	-	0.100	2.00	-	
Kaolin B	0.510	78.79	13.340	0.020	0.160	4.780	0.010	2.100	0.040	-	
Spodumene	0.360	65.20	25.130	0.150	0.050	0.210	0.100	0.340	0.570	7.50	
Zircon	-	33.00	-	-	-	-	-	-	-	-	66.0
Alumina	0.530	0.007	99.0	0.016	0.002	0.005	-	0.330	-	-	-

*Lol: loss of ignition

Tab. II Seger oxide ratios.

	SiO_2+ Al_2O_3	SiO_2 / Al_2O_3	Na_2O / K_2O	Na_2O +K_2O	Li_2O / Na_2O	Al_2O_3+ZrO_2	Opacity
STD	11.907	6.579	7.506	0.761	-	1.571	2.765
SW1	11.446	5.866	8.491	0.785	-	1.797	3.239
SW2	9.759	4.814	8.188	0.759	0.029	1.801	3.243
SW3	10.684	4.167	6.016	0.787	0.033	2.068	4.073
SW4	10.596	4.151	5.878	0.767	0.067	2.240	4.050

3.2. Phase analysis (XRD)

Fig. 2 and Table III show phase analyses and quantitative phase analyses (QPA) of the samples respectively. Mullite, quartz, albite and glassy phase were detected in STD. For

SW1, SW2, SW3 and SW4 bodies; albite, quartz and mullite embedded in glassy phase, zircon and alumina crystals were also detected. As can be seen from QPR analyses of the samples, spodumene addition contributes to increase the amount of mullite. The amount of quartz crystal in STD and SW1 bodies is higher than that of SW2, SW3 and SW4 bodies due to the fact that these bodies contain quartz. With the spodumene addition in SW2, SW3 and SW4 bodies, mullite crystals amount increased because of the fact that spodumene ($Li_2O.Al_2O_3.4SiO_2$) is highly effective fluxing agent [7-9]. The addition of spodumene is responsible for decreasing in the viscosity of the liquid phase and also results in a further quartz and albite dissolution. As can be seen in QPR analysis, the decrease in the viscosity resulted in the growth of mullite crystals and also contributed to increase in the amount of mullite crystals [7, 8]. Although the amount of the mullite crystal increased, the total amount of crystal decreased slightly compared to the STD body, because the addition of spodumene resulted in a decreased in the viscosity of liquid phase and increase in the dissolution of the albite and quartz crystals [7].

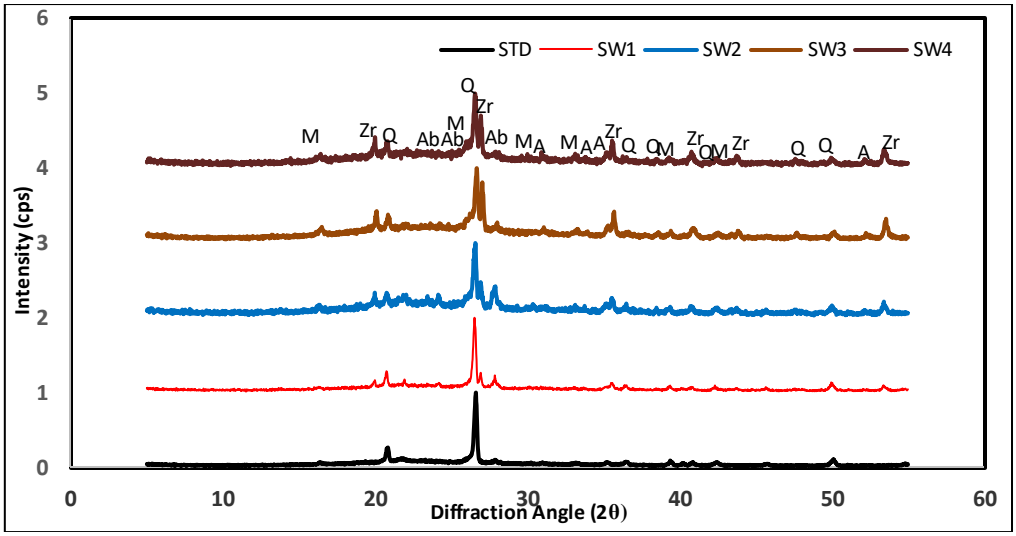

Fig. 2. XRD graphs of the fired samples, Q: Quartz, Ab: Albite, M: mullite, A: Alumina, and Zr: Zircon.

Tab. III Quantitative phase analyses of the samples.

	Quartz (%)	Albite (%)	Glassy Phase (%)	Zircon (%)	Mullite (%)	Alumina (%)	Total Crystalline Phase
STD	17.23	1.36	76,01	-	5.40	-	23.89
SW1	21.0	7.02	61.0	3.17	6.38	1.15	38.72
SW2	7.88	8.64	71.8	2.50	7.74	1.3	28.06
SW3	7.2	1.50	77.0	4.5	8.0	1.70	22.9
SW4	6.69	1.5	76.9	4.01	8.9	1.5	22,6

3.3. Technological properties

Table IV shows the technological properties of the samples. Although total porosity increased, bulk density and bending strength increased. The decrease in the viscosity of liquid phase due to the addition of spodumene resulted in a rising up in densification rate [7-10]. The decrease in the viscosity also resulted in an increase in the amount of mullite crystals [11]. The increase in the densification rate provided to obtain denser and higher strength

bodies than STD. According to literature, mullite hypothesis, the dispersion-strengthening hypothesis and the matrix reinforcement are theories explaining the strength of porcelains. Especially, mullite hypothesis explains that the strength is directly related to the interlocking of fine mullite needles in porcelain bodies [11, 12]. As can be seen Table III, the increase in amount of mullite crystals was responsible for higher strength than STD body. The addition of zircon and alumina also is responsible for higher strength bodies than STD due to their higher elastic modulus [5, 13]. The addition of zircon and alumina contributed to the increase of strength by affecting the second phase on the bodies [13-15].

CIElab method was used for colour analysis. According to this method, 3 main parameters are used to determine tile whiteness and colour. The L^* parameter refers to brightness, i.e. L: 100 means full whiteness, and L: 0 means full black. a^* parameter refers to the red-green colour range and b^* parameter refers to the yellow-blue colour range [1, 16]. The green colour is in the negative direction ($-a^*$) and the red colour is in the positive direction (a^*). The blue colour is in the negative direction ($-b^*$) and the yellow colour is in the positive direction (b^*). The whiteness of the samples SW1, SW2, SW3 and SW4 increased with the addition of zircon and alumina, while the green colour and the yellow colour slightly increased. However whiteness is the most important parameter for super white porcelain.

Tab. IV Technical results of STD, SW1, SW2, SW3, and SW4.

	Bulk Density (g/cm^3)	Bending strength (N/mm^2)	Water absorption (%)	Porosity			Colour Measurement		
				Open porosity (%) (P_O)	Closed porosity (%) (P_c)	Total porosity (%) (P_T)	**L***	**a***	**b***
STD	2.36	50	0.15	0.40	5.48	5.88	75.2	1.50	10.5
SW1	2.39	54	0.00	0.00	8.9	8.9	85.2	0.71	6.5
SW2	2.40	61	0.00	0.00	7.01	7.01	86.0	0.14	7.66
SW3	2.47	64	0.00	0.00	5.92	5.92	86.1	-0.5	7.87
SW4	2.48	70	0.01	0.00	9.02	9.02	85.8	-0.1	8.02

3.4. Solid particle erosion test and mechanical properties (SPE)

The graphs showing the mass loss, time and angles (30°, 45°, 60° and 90°) relationship obtained from the SPE is shown in Fig. 3 and Fig. 4. According to many literatures, the most important parameter affecting mass loss and/or wear rate is impingement angle [17, 18]. As can be seen in Fig. 3 and Fig. 4, although there is a linear increase in mass loss depending on time; when the angle of impact changes, the mass loss decreased after a certain angle [17, 18]. Fig. 5 shows 2D and 3D surface and crater depth graph of SW4 for different impact angle 30°, 45°, 60° and 90°. The 3D surface images of SW1, SW2, SW3 and SW4 bodies at 60° impact angle was shown in Fig. 6. Fig. 7 shows the 2D surface images of SW1, SW2, SW3 and SW4 bodies at 60° impact angle. SPE was performed according to ASTM G 76-04 [19]. Mass loss, wear rate, hardness, bending strength and elastic modulus of the samples are also given in Table V, Table VI and Table VII respectively. As seen on Fig. 3 and Fig. 4, the highest mass loss and wear rate depending on both angle and time, was observed in STD body. Especially, the increase in mullite amount with the addition of spodumene, and the addition of zircon and alumina resulted in a decrease in the mass loss and wear rate for SW1, SW2, SW3, and SW4 bodies compared to the STD body. Alumina and zircon addition have an important effect on mass loss for the developed bodies (SW1, SW2, SW3, and SW4). As seen on Table III, the body having the least total amount of alumina and zircon is SW2 body among the developed bodies. Nonetheless, the highest mass loss was observed in SW2 body among the developed bodies up to 60°. According to results of mass loss and wear rate, the wear resistance was increased in the developed bodies compared to the

STD body. Fig. 5 and Fig. 6 show that the boundaries of the erosion crater surface area are clearly visible with 3D surface maps. At all angles (15°, 30°, 45°, and 90°), samples affected by abrasive particle impingement and damage zones from which the material was removed are clearly visible in 3D surface topography images taken by a non-contact laser profilometer.

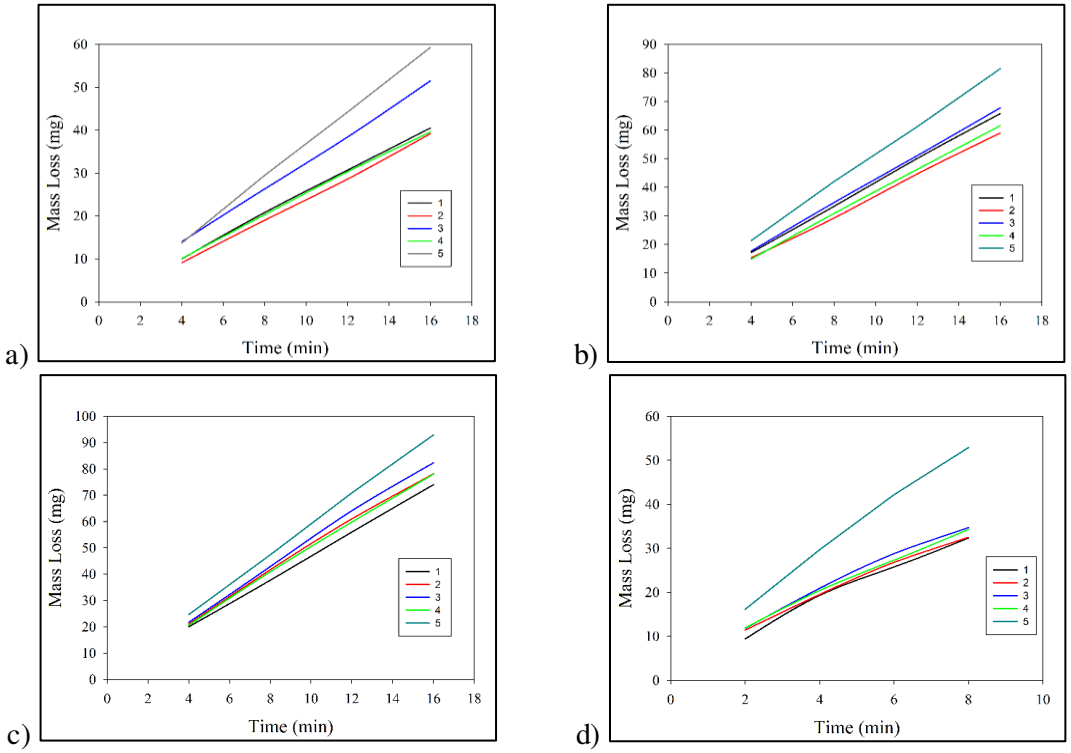

Fig. 3. Time-dependent mass loss variation for impact angles a) 30°, b) 45°, c) 60° and d) 90°, 1: SW4, 2:SW3, 3: SW2, 4: SW1, 5: STD.

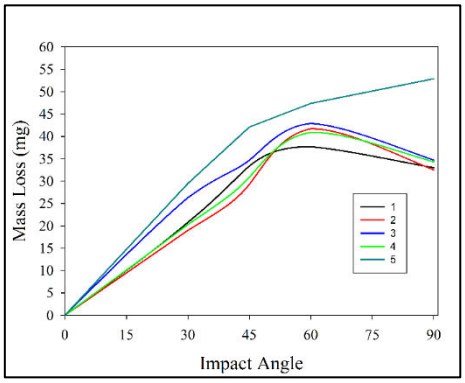

Fig. 4. Change of mass loss due to impact angle in samples; 1: SW4, 2:SW3, 3: SW2, 4: SW1, 5: STD.

However, in this study, it was determined that the wear rate did not only depend on microstructure and mechanical properties but also depended on angle of impingement. As seen in Table III, Table V and Table VI, it was found that even in bodies containing the highest ratio of the crystalline phase, the mass loss and wear rate values showed a variation depending on the impact angle. The main erosion mechanism of the ceramic bodies for lower

impact angle is due to the particle sliding. The mechanism for impact angle 90° is the peening on the flat surface [20]. Immediately after the formation of the crater (since the particles are in a vortex) it slides on its wall and continues peening only in the centre of the crater. Some authors stated that the elastic modulus of the target material seem to be an important factor in low angle impact erosion and for slurry erosion and dry impact. The increase in elastic modulus increases the rate of erosion [20]. However, in this study, it was observed that as the elastic modulus increases the rate of erosion decreases. Most of the literatures about erosion explained that materials are categorized as brittle or ductile based on the rates of erosion.

Tab. V The mass loss of the samples for 8th min.

	Mass loss(mg) for 30°	Mass loss(mg) for 45°	Mass loss(mg) for 60°	Mass loss(mg) for 90°
STD	59.3	81.5	92.9	52.9
SW1	39.6	61.6	78	34.3
SW2	51.5	67.8	82.3	34.7
SW3	39.2	59	78.1	38.25
SW4	40.5	65.8	74	32.35

Tab. VI The wear rate of the samples.

	Wear rate (mg/min) for 30°	Wear rate (mg/min) for 45°	Wear rate (mg/min) for 60°	Wear rate (mg/min) for 90°
STD	3.787	5.095	5.835	6.390
SW1	2.462	3.887	4.777	3.705
SW2	3.155	4.167	5.075	3.830
SW3	2.497	3.655	4.765	4.599
SW4	2.535	4.063	4.507	3.765

Tab. VII Hardness, Bending strength and elastic modulus of the samples.

	STD	SW1	SW2	SW3	SW4
Hardness (HV)	535	677.93	732.91	751.16	884.12
Elastic Modulus (Gpa)	60	68	74	81	83
Bending strength (N/mm^2)	50	54	61	64	70

Ductile materials (pure metals etc.) have a maximum erosion rate with low impact angles from 15° to 30°, whereas the maximum impact erosion rate is generally seen in 90° for brittle materials [21]. In this study, the maximum rate of erosion is obtained at impingement angle (90°) for STD body, which shows the brittle nature of ceramics. However, the maximum rate of erosion is obtained at impingement angle (60°) for SW1, SW2, SW3 and SW4 bodies. Erosion rate decreased at impingement angle (90°). Although ceramic materials are normally defined as brittle, the transition from brittle to ductile behaviour was observed easily. The transition to ductile behaviour occurs as soon as the wear rate decreases. Depending on the degree of wear at which erosion is maximum and/or minimum, the kind of material can be determined. The maximum wear is between 80° and 90° for brittle material. For the ductile material, the maximum wear is between 15° and 30° whereas the wear is between 45° and 60° for the semi-ductile materials [22-23]. As seen on Fig. 4, after 60°, semi ductile behaviour was observed in SW1, SW2, SW3 and SW4 bodies [22-25]. But, STD body showed brittle behaviour. In this study, it was showed that the combination of spodumene,

zircon and alumina increased the abrasion resistance of porcelain stonewares and the brittle nature of the porcelain stonewares is made semi ductile. This was confirmed by maximum erosion at 60° [22-24]. As can be also seen in Table VII, the addition of high elastic modulus materials, such as alumina and zircon, together with the spodumene increasing the amount of mullite contributed to increase hardness, elastic modulus and strength approximately 30-40 %.

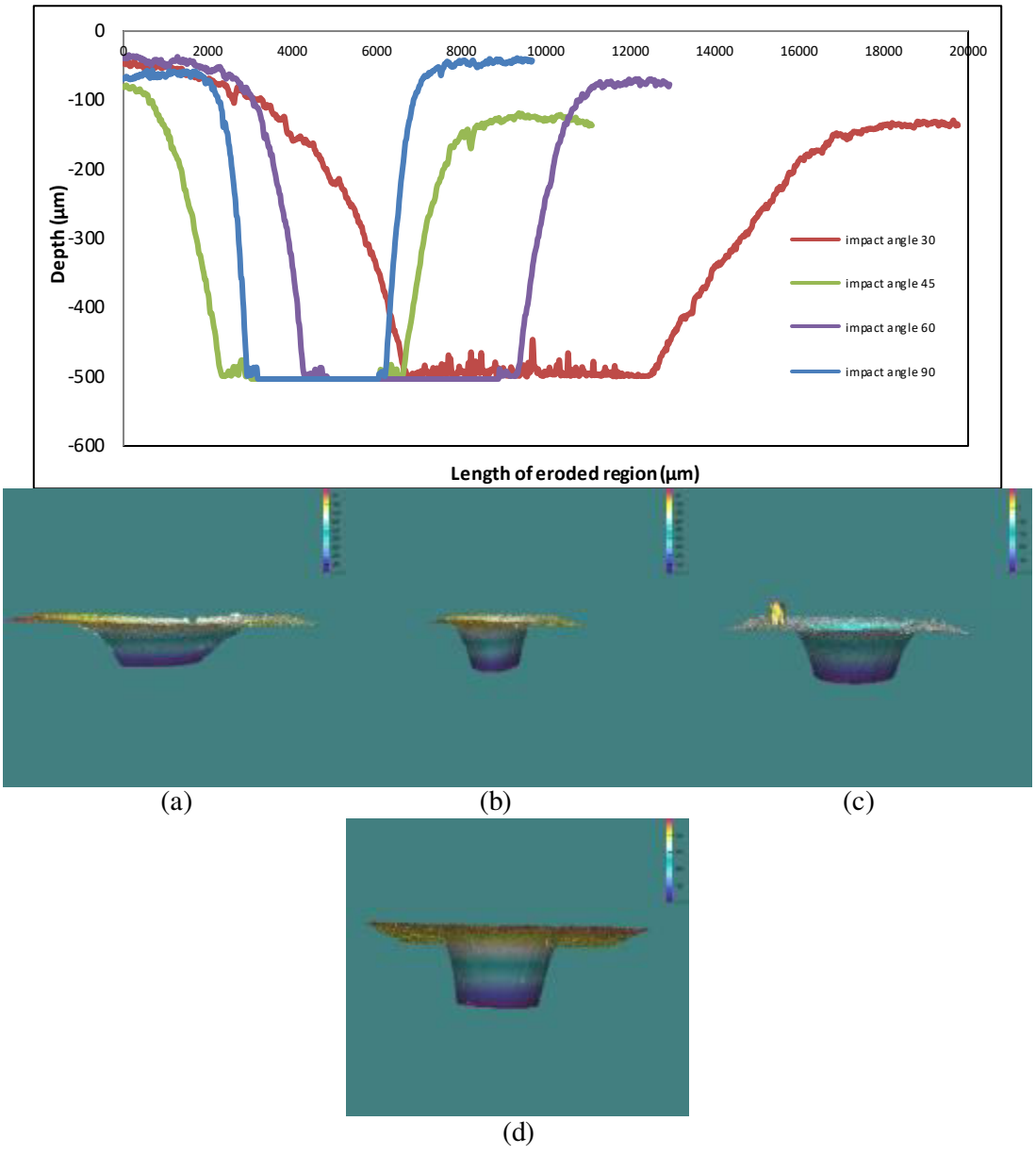

Fig. 5. 2D and 3D Surface and crater depth graph of SW4 for different impact angle a) 30° b) 45° c) 60° and d) 90°.

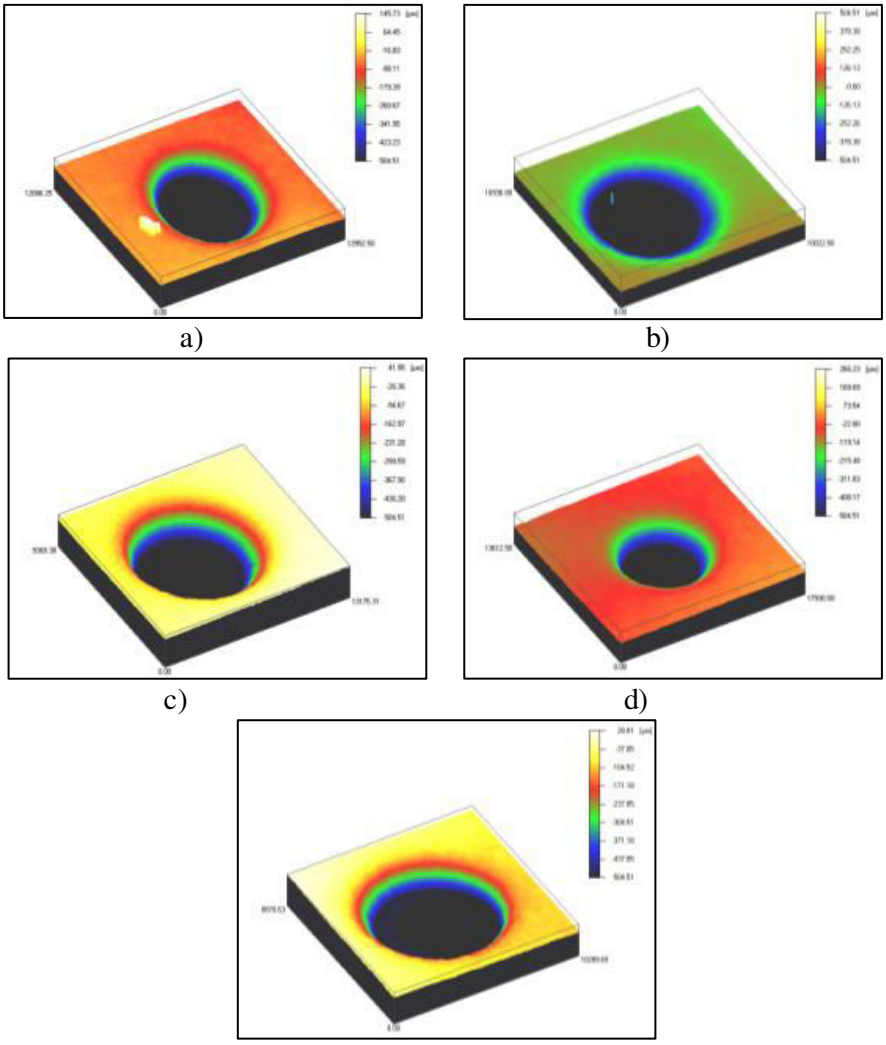

Fig. 6. The 3D surface images of samples at 60^0 impact angle for different samples a) SW4 b) SW3 c) SW2 and d) SW1 e) STD.

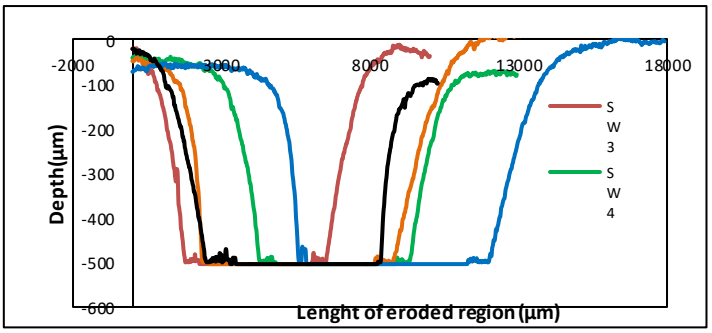

Fig. 7. The 2D surface images of samples at 60° impact angle for SW1, SW2, SW3, SW4 and STD.

3.5. Microstructural analysis (SEM)

SEM and EDX micrographs of the samples are shown in Fig. 8. All images include both impingement surface and etched surface. Mullite, quartz and the glassy phase were

detected for all samples. Pores are also seen in microstructure due to solid impingement test. Primary Mullite (PM) crystals defined as cuboidal crystals from clay agglomerate relicts [7, 12, 26]. Secondary Mullite (SM) characterised as elongated needle-shaped crystals from Primary Mullite crystals [27]. As mentioned before, the addition of alumina and zircon together with the spodumene increasing mullite crystals contributed to increase hardness, elastic modulus and strength [28]. Both needles and cuboidal mullite crystals are common in all bodies. The white coloured crystals seen in the images are zircon crystals.

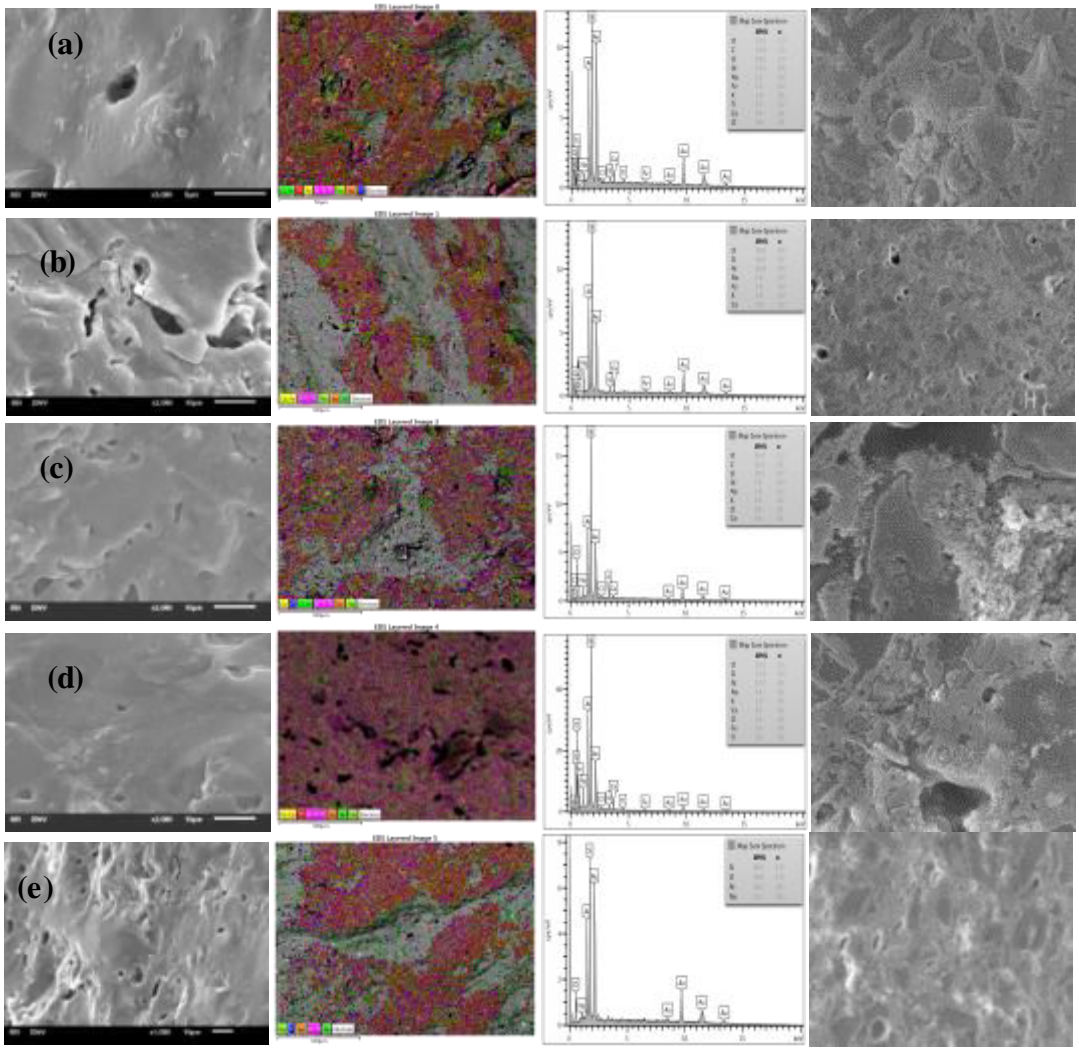

Fig. 8. SEM and EDX micrograph of (a): STD, (b): SW1, (c): SW2, (d): SW3, (e): SW4.

4. Conclusion

In this study, the optical, mechanical and microstructural properties of the porcelain stoneware bodies were investigated. In order to improve the porcelain stoneware properties the certain ratio of spodumene, alumina and zircon were added in the composition. The addition of spodumene, alumina and zircon improved the technological, mechanical and microstructural properties. Bulk density increased while water absorption decreased. With the addition of zircon and alumina whiteness of the developed samples increased due to their

opacifying effect. Hardness, bending strength and elastic modulus increased. Hardness, bending strengths and elastic modulus increased approximately 30-40 % compared to the standard body. Wear resistance was improved compared to standard body. Although ceramics are known as brittle, they have been shown to exhibit semi ductile behaviour depending on the angle of impact and the addition of spodumene, zircon and alumina. As soon as the impact angle of the developed samples exceeded 60°, it was found that wear rates decreased immediately due to semi ductile behaviour. However, standard body did not exhibit any ductile behaviour. STD body exhibits brittle behavior for all impact angles.

5. References

1. N. T. Selli, Development of anorthite based white porcelain stoneware tile compositions, Ceram. Int., 41 (2015) 7790-7795.
2. C. Siligardi, P. Miselli, L. Lusvarghi, M. Reginelli, Influence of CaO-ZrO_2-Al_2O_3-SiO_2 glass-ceramic frits on the technological properties of porcelain stoneware bodies, Ceram. Int., 37 (2011) 1851-1858.
3. E. Rambaldi, A. Tucci, L. Esposito, D. Naldi, G. Timellini, Effects of nano-oxides on the surface properties of ceramic tiles, Bol. Soc. Esp. Ceram. V. 49, 4 (2010) 253-258. http://www.qualicer.org/recopilatorio/ponencias/pdfs/2010143.pdf.
4. K. Karaveli, B. Karasu, H. S. Onal, Production of zircon-free opaque wall tile frits and their use in ceramic industry, Conference: Qualicer 2008, Castellon, Spain https://www.researchgate.net/publication/258909610_Production_of_Zirconfree_Opaque_Wall_Tile_Frits_and_Their_Use_in_Ceramic_Industry.
5. W. H. Gitizen, Mechanical Properties of Alumina, Alumina as a ceramic material, Wiley, 43-44, 1970.
6. W. H. Gitizen, Optical Properties of Alumina, Alumina as a ceramic material, Wiley, 89, 1970.
7. T. Aydin, Investigation of stain resistance of porcelain stonewares doped by spodumene, (Ph.D. thesis), Anadolu University, Eskisehir, Turkey, 2012.
8. T. Aydin, O. Bican, R. Gümrük, Investigation of wear resistance of the porcelain stoneware bodies by solid particle impingement using alumina particles, Journal of the Australian Ceramic Society, 56, (2020) 525-531.
9. M. Oberzan, High-alumina porcelain with the addition of a Li_2O-bearing fluxing agent, J. Eur. Cer. Soc., 29(11) (2009) 2143-2152.
10. D. U. Tulyaganov, S. Agathopoulos, H. R. Fernandes, J. M. F. Ferrea, Influence of lithium oxide as auxiliary flux on the properties of triaxial porcelain bodies, J. Eur. Cer. Soc., 26 (2006) 1131-1139.
11. T. Aydin, N. Kunduracı, A. Akbay, The effect of nepheline syenite addition on pyroplastic deformation of sanitarywares, Science of Sintering, 50, 1 (2018) 85-94.
12. P. Ranachowski, F. Rejmund, Z. Ranachowski, A. Pawelek, A. Piatkowski, S. Kudela Jr, Evaluation of the mullite hypothesis in respect of electrotechnical porcelains, Archives of Metallurgy and Materials, 58 (4) (2013) 1177-1181.
13. T. Aydin, A. Kara, Effects of Alumina on Porcelain Insulators, Journal of the Aust. Ceram. Soc. 52, 1 (2016) 83-88.
14. T. Aydin, M. Tarhan, B. Tarhan, Addition of cement kiln dust in ceramic wall tile bodies, J. Ther. Analy. and Calori, 136 (2019) 527-533.
15. T. Aydin, C. Paksoy, The Effect of Cement Raw Mix Waste Dust on Porcelain stoneware Properties, J. Aust. Ceram. Soc 55 (2019) 37-45.
16. M. Tarhan, Whiteness improvement of porcelain stonewares incorporated with anorthite and diopside phases, J. Ther. Anal. Calori., 138 (2019) 929-936.

17. H. Arabnejad , A. Mansouri, S.A. Shirazi, B.S. McLaury, Abrasion erosion modelling in particulate flow, Wear, 376-377 (2017) 1194-1199.
18. Y. I. Oka, M. Nishimura, K. Nagahashi, M. Matsumura, Control and evaluation of particle impact conditions in a sand erosion test facility, Wear, 250 (2001) 736-743.
19. ASTM G76-04, Standard Test Method for Conducting Erosion Tests by Solid Particle Impingement Using Gas Jets1.
20. K. R. Gopi, R. Nagarajan , S. S. Rao, S. Mandal, Erosion model on alumina ceramics: A retrospection, validation and refinement, Wear 264 (2008) 211-218.
21. X. Wang, M. Fang, L. C. Zhang, H. Ding, Y. G. Liu, Z. Huang, S. Huang, J. Yang, Solid particle erosion of alumina ceramics at elevated temperature, Materials Chemistry and Physics, 139 (2013) 765-769.
22. M. G. Yilmaz, H. Unal, A. Mimaroglu, Study of the strength and erosive behavior of $CaCO_3$/glass fiber reinforced polyester composite, eXPRESS Polymer Letters, 2, 12 (2008) 890-895.
23. G. Raghavendra, S. Ojha, S. K. Acharya, S .K. Pal, Jute fiber reinforced epoxy composites and comparison with the glass and neat epoxy composites, Journal of Composite Materials, 48, 20 (2014) 2537-2547.
24. J. R. Mohanty, S. N. Das, H. C. Das, T. K. Mahanta, S. B. Ghadei, Solid Particle Erosion of Date Palm Leaf Fiber Reinforced Polyvinyl Alcohol Composites, Advances in Tribology, Volume 2014, Article ID 293953 (2014) 1-8. https://doi.org/10.1155/2014/293953
25. Brian R. T., Tribology of ceramics, National academy process, 1988 National Research Council (U.S.). Committee on Tribology of Ceramics.
26. J. M. Pérez, M. Romero, Microstructure and technological properties of porcelain stoneware tiles moulded at different pressures and thicknesses, Ceramics International, 40 (2014) 1365-1377.
27. D. Wei, H. Y. He, High Strength Glass-Ceramics Sintered With Coal Gangue as a Raw Material, Science of Sintering, 51, 3 (2019) 285-294.
28. B. Ngayakamo, S. E. Park, Evaluation of Kalalani Vermiculite for Production of High Strength Porcelain Insulators, Science of Sintering, 51, 2 (2019) 223-232.

Сажетак: *Нови систем производње развијен у последњих неколико година је довео до могућности побољшања естетског изгледа великих производа од порцелана. Да би се добиле такве плоче, оптичка и механичка својства треба да буду побољшана. Та својства су повезана са микроструктуром. У овом раду, сподумен, алумина и цирконијум су коришчени да би се побољшала микроструктура порцелана а тиме и оптичка и механичка својства. Отпорност на хабање је једна од најзначајнијих механичких својстава. Коришћени су различити методи анализе отпорности на хабање. Методом удара употребом честица алумине одредила се отпорност на хабање производа од порцелана.*

Кључне речи*: порцелан, метода удара, отпорност на хабање, оптичка својства.*